A New Energy Building Simulation Library

Juan I. Videla Bernt Lie
Telemark University College
Department of Electrical Engineering, Information Technology, and Cybernetics
Porsgrunn, 3901 Norway

Abstract

Due to the increased interest in saving energy in buildings, new dynamic building models that describe transient response in more flexible modeling languages become necessary. Following some ideas from a previous building thermal behavior library written in Modelica, a new library for modeling building thermal response is presented. The library is meant for system level simulation and its basic elements consist of lumped and one-dimensional distributed parameter models. Object-oriented features like class parameters, inheritance, and aggregation are extensively used to improve the library structure making it easy to read and use. Complex building topologies can be built-up from component models that can be efficiently simulated and studied in any Modelica simulation environment. A comparative test using BESTEST (Building Energy Simulation Test) is performed for inter-program comparison with traditional whole building energy simulation environments.
Keywords: building modeling; building energy simulation; inter-program comparison

1 Introduction

Buildings are complex nonlinear dynamic systems that involve many physical aspects – heat conduction, convective flow, radiation, mass flows, etc.– with hundreds of variables and parameters that must be properly addressed. Due to the complexity and highly coupled nature of these phenomena, simulation seems to be the most cost effective way to study how to improve the energy efficiency in buildings [1]. Although there are many building energy simulation tools available [11], [2], the majority of them are not convenient to easily test and develop advanced controllers and supervisory control techniques.
The hierarchical structure of buildings allows the definitions of different levels of detail naturally. So a building can be divided into different levels going from physical phenomena components to more complex structures like the building itself. A basic elements sublibrary for lumped and distributed parameter models can be defined to represent the underlying physical phenomena. More complex elements are naturally derived from these basic components. Depending on the complexity and the requirements of the problem the models can be adapted and several building topologies can be easily assembled.

The building library, HITLib, is evaluated using BESTEST comparative testing procedure [6] with a special emphasis in the models required to represent the test cases. HITLib is also capable to represent inter-zone convective energy flows in multi-zone buildings using mass and energy balances for the lumped control volumes which represent rooms, and steady-state hydraulic fluid assumption for the bidirectional mass flow components like cracks, doors, ventilations, etc.
In the next section, a general overview of the library structure is given. Then, the main building models used in the test cases are developed. The BESTEST inter-program comparison results are presented in section 4. To sump up with the conclusions and future work in the last section.

2 Library overview

The library is organized in 6 main packages (see figure 1)

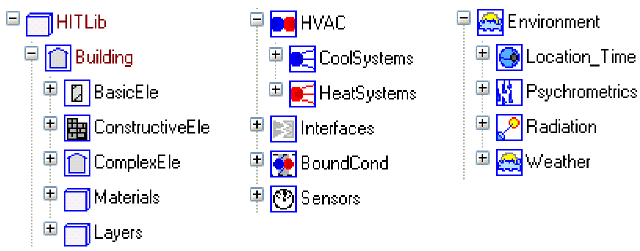

Figure 1: HITLib general library structure.

- Building – Basic, Constructive, and Complex elements; material properties and layers geometry sublibraries
- Environment – Location_Time, Psychrometric, Solar radiation, and Weather sublibraries
- HVAC – Heating, Ventilating and Cooling Systems sublibraries
- Interfaces – all connectors and components used in interconnections.
- BoundCond – Variable and fixed sources and sinks according to the connectors.
- Sensors – Sensor models for the different external interfaces (connectors)

Basic models generally described elementary models like the air heat and mass storage in a control volume, the orifice equation, single and multilayer conductive models, convective models, and radiation exchange models. Many of the basic model formulations found in HITLib are similar to the ones found in ATPlus library [4], while other ones give a more detailed description of the underlying phenomena (e.g. longwave radiation exchange in the enclosure model, air mass storage, orifice equation, etc.).

Constructive models like a wall model are built by combining basic models. For instance, a wall component addressing radiation, multi-layer conduction and convection is constructed through aggregation and inheritance of basic models. In a similar way, ventilations, doors, windows, roofs, floors, junctions, cracks, etc. can be defined from the basic models.

Complex elements like a room (see Fig. 5) or a storey are defined by aggregation of constructive elements. They are basically template-like components where the subcomponents constructive element parameters are directly defined through the complex element higher level parameters. In this way, the material used in the walls of a room can be directly defined through the higher level room parameters.

Materials subpackage contains records of different material properties. In general parameters are grouped in partial models to increase readability and reuse in similar components at each level.

Environment subpackage contains models and functions to calculate solar radiation and position, perform psychrometric conversions, estimate sky-temperature, and load and interpolate weather data files in tables.

HVAC subpackage contains models representing electrical heaters, radiators, valves, pipes, boilers, pumps, chillers, heat exchangers, etc.

BoundCond and Sensor libraries defined all possible interactions with the connectors used in the different models. Icons are defined in the Icons package and they are inheritated in the library models to increase model readability.

3 Building models description

The thermal response of a building space include the heat transfer from the enclosing walls and roofs through conduction and convection, solar heat gains through windows, heat gains or losses due to infiltration, internal long wave exchange and internal short wave absorption and distribution among the enclosure surfaces, and short wave heat gains from internal sources. Additionally, the exterior wall exchange heat with the environment through convection, longwave radiation, and shortwave absorption. The air within a room is represented through a lumped control volume connected to the internal convective sides of the inner surfaces of the envelope.

3.1 Air volume model

HITLib has three different models to represent the air volume within a room.

An air volume model formulated using a dynamic mass and internal energy balances within a lumped control volume,

$$\begin{aligned} \frac{dm(t)}{dt} &= \sum_j \dot{m}_j(t) \\ \frac{dU(t)}{dt} &= \sum_j \dot{H}_j(t) + \sum_k \dot{Q}_k(t) \\ H(t) &= U(t) + p(t)V(t) \\ H(t) &= m(t)h(t) \\ U(t) &= m(t)u(t) \end{aligned} \tag{1}$$

where m is the mass within the control volume, $\dot{m}_j$ the mass in/outflows, $\dot{H}_j$ the enthalpy in/outflows, $\dot{Q}_k$ the heat in/outflows, U the internal energy, H the enthalpy, p the pressure, V the volume, and h and u, the specific enthalpy and specific internal energy, respectively. The ideal gas law is used since nominal temperatures, pressures, and densities for buildings are well within the range of validity of this thermodynamic model. The ideal gas law is implemented in a partial model class, and used when necessary in other components through inheritance. The preferred states and their initial conditions are then selected, and model reformulation is automatically done by Dymola using its built-in symbolic math capabilities for dealing with DAE (Differential Algebraic Equations):

$$\begin{aligned} p(t)v(t) &= RT(t) \\ u(t) &= u_0 + c_v(T(t) - T_0) \\ h(t) &= u(t) + p(t)v(t) \end{aligned} \tag{2}$$

where, v is the specific volume, T the temperature, u_0 the specific internal energy at T_0, and R the gas constant. This air volume model is also extended in the AirVolHum model to account the

A more basic air volume model represented as a simple heat storage unit (the model that has been used in the BESTEST analysis) is

$$\dot{Q}_{\text{air}} = c_{p\text{air}} \rho_{\text{air}} V_{\text{room}} \frac{dT_{\text{air}}}{dt} \tag{3}$$

where $c_{p\text{air}}$ is the air specific heat capacity, ρ_{air} is the air densitiy, V_{room} is the air volume, $\dot{Q}_{air}$ is the net heat flow rate entering the air volume, and T_{air} is the air temperature within the volume.

Additionaly, a model that accounts the humidity variation within the air volume formulated from a dynamic mass and internal energy balances is available.

3.2 Exterior and interior wall heat transfer models

The heat transfer that takes place at each exterior surface (or roof) i on the outside of building can be calculated using the following heat balance

$$\dot{Q}_{\text{cond},i} = \dot{Q}^o_{\text{conv},i} + \dot{Q}^o_{\text{radsol},i} + \dot{Q}^o_{\text{radlw},i} \tag{4}$$

where $\dot{Q}_{\text{cond},i}$ is the conduction heat flow rate between the external surface and the inner conductive layers, $\dot{Q}^o_{\text{conv},i}$ is the convective heat transfer between the outdoor air and the wall surface, $\dot{Q}^o_{\text{radsol},i}$ is the heat flow rate that the external surface of a wall or roof absorbs from the total incident solar radiation, $\dot{Q}^o_{\text{radlw},i}$ is the heat flow rate from the long wave radiation that the external surface exchanges with the surroundings, such as outdoor air, the ground and nearby buildings, and the sky.

With

$$
\begin{aligned}
\dot{Q}^{o}_{\mathrm{conv},i} &= h_o\left(T_{\mathrm{out}}-T_{\mathrm{sur},i}\right)\\
\dot{Q}^{o}_{\mathrm{radsol},i} &= A_i\alpha_i\left(I_{\mathrm{dif},i}+I_{\mathrm{dir},i}\right)\\
\dot{Q}^{o}_{\mathrm{radlw},i} &= \varepsilon_i\sigma\Big[F_{\mathrm{air}}\left(T^4_{\mathrm{out}}-T^4_{\mathrm{sur},i}\right)+\\
&\quad F_{\mathrm{g}}\left(T^4_{\mathrm{g}}-T^4_{\mathrm{sur},i}\right)+F_{\mathrm{sky}}\left(T^4_{\mathrm{sky}}-T^4_{\mathrm{sur},i}\right)\Big]
\end{aligned}
\tag{5}
$$

where h_o is the convective heat transfer coefficient of the external wall surface, T_{out} is the outside temperature, $T_{\mathrm{sur},i}$ is the wall surface temperature, α_i is the shortwave absorptivity, $(I_{\mathrm{dif},i}+I_{\mathrm{dir},i})$ is the total incident solar radiation (direct and diffuse radiation impinging the external surface), A_i is the area of incidence of the solar radiation, ε_i is the outer layer emissivity, σ is the stefan-boltzmann constant, F_{air} is the surface-air view factor, F_{g} is the surface-ground view factor, T_{g} is the ground temperature, F_{sky} is the surface-sky view factor, and T_{sky} is the sky temperature.

The one dimensional heat conduction through an homogeneous isotropic solid (e.g. layer of a wall) $\dot{Q}_{\mathrm{cond},i}$, with material properties independent of temperature, can be modeled as a one dimensional PDE of the form:

$$
\begin{aligned}
\dot{Q}_{\mathrm{cond}} &= -kA_{\mathrm{cond}}\partial T/\partial x\\
\partial T/\partial t &= \tfrac{1}{\rho c}\partial\dot{Q}_{\mathrm{cond}}/\partial x
\end{aligned}
\tag{6}
$$

where T is the temperature, $\dot{Q}_{\mathrm{cond}}$ is the conductive heat flow rate, A_{cond}, k, ρ, and c are conductive area, thermal conductivity, density and specific heat capacity of the material, respectively. This equation can be solved using the method of lines (i.e. spatial discretization), see the following Modelica code fragment from the single layer model **CondM1:**

```
model CondM1
 ...
equation
 for i in 2:Ndis loop
   Area*dx*Material.rho*Material.c*der(T[i]) = Q[i - 1] - Q[i];
 end for;
 for i in 2:Ndis + 1 loop
   Q[i - 1] = (Material.lambda*Area)*(T[i - 1] - T[i])/dx;
 end for;
...
end CondM1;
```

The single layer component **CondM1** can be extended to the multilayer case **CondMc** by declaring it n times, each declared single layer component is interconnected using a for clause and the connect command as shown below:

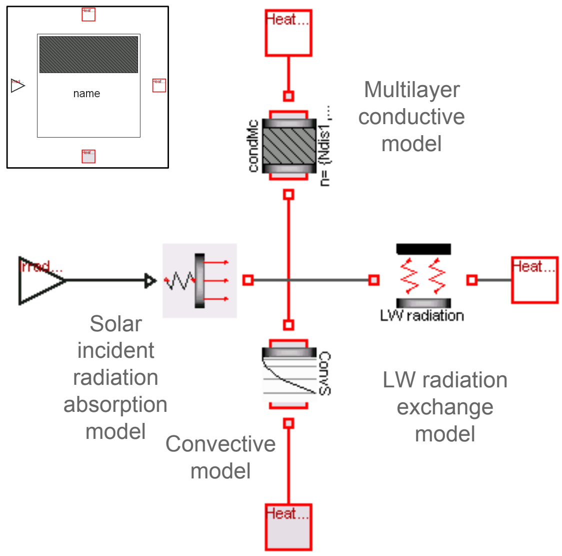

Figure 2: Half exterior roof model icon and diagram layer.

```
model CondMc
...
 CondM1 CondM[Nlay](
   Area=Area[1:Nlay],
   Ndis=Ndis[1:Nlay],
   Len=Len[1:Nlay],
   Tini=Tini[1:Nlay],
   Material=Material[1:Nlay]);
  equation
  connect(CondM[1].Heat_a, Heat_a);
  connect(CondM[Nlay].Heat_b, Heat_b);
  for i in 1:Nlay - 1 loop
    connect(CondM[i].Heat_b, CondM[i + 1].Heat_a);
  end for;
end CondMc;
```

Finally, more complex models (e.g. constructive models like wall, roof, or floor models) can be built aggregating convective models and the multilayer conductive model **CondMc**. As an example see the diagram layer of the half exterior roof model in Fig. 2. The additional models represent the heat flow rate $\dot{Q}^{o}_{\mathrm{radsol},i}$, that the external surface of the roof absorbs from the total incident solar radiation impinging the exterior surface, and the long wave radiation heat flow rate $\dot{Q}^{o}_{\mathrm{radlw},i}$, that the external surface exchanges with the sky for this particular model. This exterior half roof model represents the heat balance at the exterior side of a building roof. This model has azimuth and tilt angle parameters to properly define the total solar radiation. Similarly, other constructive models can be defined by aggregation of elemetary models and class parameters of the inner models.

A similar heat balance can be formulated for each building wall (or roof) interior surface i within the building

$$
\dot{Q}_{\mathrm{cond},i}+\dot{Q}^{i}_{\mathrm{conv},i}+\dot{Q}^{i}_{\mathrm{radsw},i}+\dot{Q}^{i}_{\mathrm{radlw},i}=0 \tag{7}
$$

where $\dot{Q}_{\mathrm{cond},i}$ is the conductive heat transfer between the wall inner layers and the internal wall surface of the room,

$\dot{Q}^i_{\text{conv},i}$ is the convective heat transfer between the internal air and the wall surface, $\dot{Q}^i_{\text{radsw},i}$ is the heat flow rate that the internal outer surface of a wall or roof would absorb from any short wave source (e.g. incoming solar radiation from the window model or short wave radiation from a bulb model), and $\dot{Q}^i_{\text{radlw},i}$ is the net heat flow rate due to the long wave radiation exchange among the internal surfaces.

$$\begin{aligned}\dot{Q}^i_{\text{conv},i} &= h_i\left(T_{\text{int}} - T_{\text{sur},i}\right)\\ \dot{Q}^i_{\text{radsw},i} &= Fa_i\dot{Q}_{\text{wind}}\\ \dot{Q}^i_{\text{radlw},i} &= A_{\text{sur},i}\frac{\varepsilon_i}{1-\varepsilon_i}\left(\sigma T^4_{\text{sur},i} - J_{\text{sur},i}\right)\\ \dot{Q}^i_{\text{radlw},i} &= A_{\text{sur},i}\sum_{j=1}^{N} F_{i,j}\left(J_{\text{sur},i} - J_{\text{sur},j}\right)\end{aligned} \quad (8)$$

where h_i is the convective heat transfer coefficient of the internal wall surface i, T_{int} is the air volume temperature, Fa_i is the internal solar distribution fraction (for details see Kreith and Bohn (1993)), $\dot{Q}_{\text{wind}}$ is the heat flow rate from the incoming solar radiation into the enclosure through the windows, $J_{\text{sur},i}$ is the radiosity of surface i, $J_{\text{sur},j}$ is the radiosity of surface j, $F_{i,j}$ is the view factor between surfaces i and j, and N is the number of enclosure surfaces.

The long wave radiation exchange among the surfaces of the enclosure has been implemented in the **enclosure** model. The conventional radiation heat transfer network analysis method [10] has been used assuming plain gray diffuse surfaces. The **enclosure** model is included in the **room42_B** model and each radiating surface is separately connected to the enclosure model using a connector array. The view factors depend on the geometry, position, and surface emissivity of each of the inner surfaces of the enclosure, they can be precalculated and loaded or an area weighted approach can be directly calculated in the component.

The shortwave radiation distribution is implemented with a model that uses precalculated solar fractions according to the geometry and absorptivity of the internal surfaces.

3.3 Windows heat transfer model

The window model (see Fig. 3) is also built from basic models by aggregation, the heat transfer through a window can be approximated by three parts,

- a conductive-convective part due to the temperature difference between the exterior and interior of the building,
- a solar heat gain model due to the solar radiation,
- and a convective energy flow due to infiltration.

The Window model used to evaluate HITLib with BESTEST do not include any infiltration or ventilation component driven by pressure differences between zones. The building infiltration is directly represented using a simpler ASHRAE model in the room model.

The conductive-convective heat transfer part due to the temperature difference between the exterior and interior of the building is modeled using two convective models for the external surfaces at both sides of the windows, and a conductive model representing the glass pane. This part of the Window model represents the rate of heat transfer through

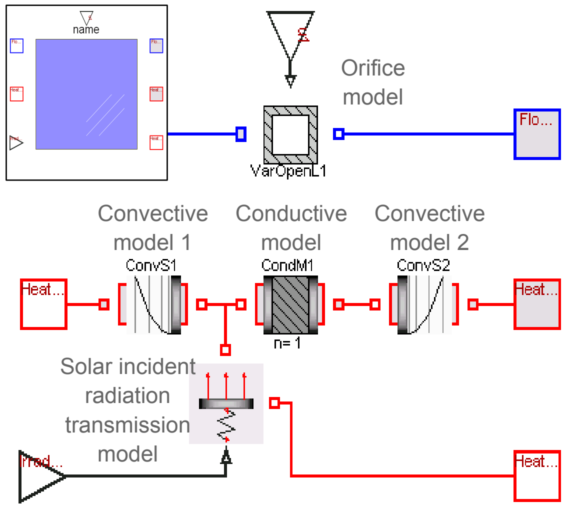

Figure 3: Window model icon and diagram layer.

the windows in the absence of sunlight and air infiltration. Multi-glass windows can be approximated by this simplified model or otherwise, the model can be easily extended to account for a multi-pane window. The total solar heat flow rate trough the glass is calculated with the solar incident radiation transmission model.

3.4 Infiltration heat transfer model

The infiltration heat transfer model represents the building's sensible thermal load due to air exchange by infiltrations. The incoming air must be heated or cooled depending on the temperature difference between the outdoor and indoor air. The heat flow rate due to this sensible heating or cooling is given by

$$\dot{Q}_{\text{inf}} = I_{\text{ACH}} V_{\text{room}} \rho_{\text{air}} c_{p\text{air}} \left(T_{\text{out}} - T_{\text{int}}\right) \quad (9)$$

where $\dot{Q}_{\text{inf}}$ is the sensible heat load, ρ_{air} is the air density, $c_{p\text{air}}$ is the specific heat of air, V_{room} is the room volume, I_{ACH} is the air exchange rate also called air changes per hour (ACH), T_{out} is the outside temperature, and T_{int} is the indoor temperature. The infiltration model can be seen in the diagram layer of the **room42_B** model in Fig. 5

3.5 Environment model

The environment model calculates the sun position and solar radiation with respect to and over each exterior building surface (for a detailed description of the following equations see [5], [3], [9], and [8]). The environment model diagram layer used with the BESTEST simulations can be seen in Fig. 4. Subcomponents (1), (2), (3), and (4) are used to calculate the solar time t_{sol}, the hour angle ω, and the solar declination angle δ (angle between the earth's equatorial plane and the sun beam in the selected location),

$$
\begin{aligned}
t_{\mathrm{sol}} &\triangleq t_{\mathrm{std}} + \frac{L_{\mathrm{std}}-L_{\mathrm{loc}}}{15^\circ/\mathrm{h}} + \frac{E_t}{60\,\mathrm{min/h}} && (10)\\
\omega &= \frac{\pi(t_{\mathrm{sol}}-12\,\mathrm{h})360^\circ}{24\,\mathrm{h}180^\circ} && (11)\\
E_t &= 9.87\sin(2a) - 7.53\cos(a) - 1.5\sin(a) && (12)\\
a &= \frac{360^\circ(n-81)}{364} \\
\sin(\delta) &= -\sin\left(\frac{23.45^\circ\pi}{180}\right)\cos\left(2\pi\frac{n+10}{365.25}\right) && (13)
\end{aligned}
$$

where t_{sol} is the solar time, t_{std} is the standard time, L_{std} is the standard longitude, L_{loc} is the local longitude, E_t is the equation of time, and n is the day of the year.

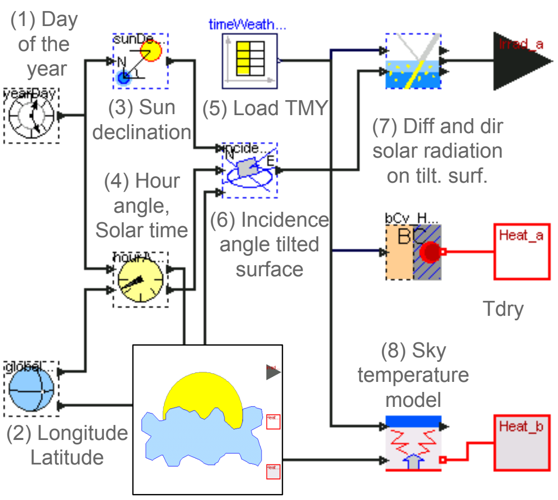

Figure 4: Environment model used with BESTEST analysis.

Subcomponent (6) in Fig. 4 calculates the solar incidence angles θ_i for arbitrary planes i in terms of the tilt θ_{sur} and the azimuth ϕ_{sur} angles of the surface normal,

$$
\begin{aligned}
\cos\theta_i = {} & \cos\theta_{\mathrm{sur}}(\cos\delta\cos\omega\cos\lambda_{\mathrm{lat}} + \sin\delta\sin\lambda_{\mathrm{lat}}) \\
& + \sin\theta_{\mathrm{sur}}\sin\phi_{\mathrm{sur}}\cos\delta\sin\omega \qquad (14)\\
& + \sin\theta_{\mathrm{sur}}\cos\phi_{\mathrm{sur}}(\cos\delta\cos\omega\sin\lambda_{\mathrm{lat}} \\
& - \sin\delta\cos\lambda_{\mathrm{lat}})
\end{aligned}
$$

where λ_{lat} is the building latitude (obtained from subcomponent (2) in Fig. 4). In the current implementation the incidence angle θ_i is calculated for the following surface tilt angles $\theta_{\mathrm{sur}} = (0^\circ, 45^\circ, 90^\circ)$ that correspond to horizontal surface, 45° tilted surface, and a vertical surface; and for the following surface azimuth angles $\phi_{\mathrm{sur}} = (180^\circ, 135^\circ, 90^\circ, 45^\circ, 0^\circ, -45^\circ, -90^\circ, -135^\circ)$ that correspond to North, North-east, East, South-East, South, South-west, West, and North-West directions. In this way 17 different incidence angles are obtained for the 24 different combinations of surface tilt and azimuth angles[1].
The Load TMY model (see subcomponent (5) in Fig. 4) loads the hourly TMY weather data file into a table. The table entries include the dry temperature T_{dry}, the dew point temperature T_{dp}, the atmospheric pressure p, the relative humidity H_{rel}, the wind velocity W_{vel}, the wind direction W_{angle}, the global horizontal radiation $H_{glo,hor}$,the diffuse horizontal radiation $H_{dif,hor}$, the total sky cover n_{to}, the opaque sky cover n_{op} and the ceiling height h.
For every incidence angle θ_i, the diffuse solar radiation over a tilted surface $H_{\mathrm{diftil},i}$ and the direct solar radiation over a tilted surfaces $H_{\mathrm{dirtil},i}$ are calculated from the hourly global horizontal radiation $H_{glo,hor}$ and the hourly diffuse horizontal radiation $H_{dif,hor}$,

$$
\begin{aligned}
H_{dir,hor} &= H_{glo,hor} - H_{dif,hor} && (15)\\
H_{\mathrm{dirtil},i} &= \frac{H_{dir,hor}}{\cos\theta_s}\cos\theta_i && (16)\\
H_{\mathrm{diftil},i} &= H_{dif,hor}\frac{1+\cos\theta_{\mathrm{sur}}}{2} \\
&\quad + H_{glo,hor}\rho_{gro}\frac{1-\cos\theta_{\mathrm{sur}}}{2} && (17)
\end{aligned}
$$

where ρ_{gnd} is the ground reflectance.
Finally the sky temperature model (see subcomponent (8) in Fig. 4) based on [7] model estimates the sky temperature T_{sky}. First the clear sky emissivity $\varepsilon_{\mathrm{clear}}$ is calculated from the dew point temperature T_{dp}, the solar time t_{sol}, the atmospheric pressure P as

$$
\begin{aligned}
\varepsilon_{\mathrm{clear}} = {} & 0.711 + 0.56\left(\frac{T_{\mathrm{dp}}}{100}\right) + 0.73\left(\frac{T_{\mathrm{dp}}}{100}\right)^2 + \\
& 0.013\cos\left(\frac{2\pi t_{\mathrm{sol}}}{24}\right) + 0.00012(P-1000) \qquad (18)
\end{aligned}
$$

the sky emissivity ε is calculated from the clear sky emissivity and the cloud amount C, which is estimated using the following equations,

$$
\begin{aligned}
\varepsilon &= \varepsilon_{\mathrm{clear}} + (1-\varepsilon_{\mathrm{clear}})C && (19)\\
C &= \sum n_i \varepsilon_{c,i} \Gamma_i && (20)\\
\ln\Gamma_i &= -h_i/h_0 && (21)
\end{aligned}
$$

where n_i is the sky cover fractional area for each cloud layer i, $\varepsilon_{c,i}$ is the hemispherical cloud emissivity for each cloud layer i, Γ_i is a factor that depends on the cloud base temperature for each cloud layer i and can be approximated by equation 21 where h_i is the cloud layer base height and h_o is equal to 8200 m. Finally, the black-body sky temperature is computed as

$$
T_{\mathrm{sky}} = \varepsilon^{\frac{1}{4}} T_{\mathrm{db}} \qquad (22)
$$

3.6 Room model

The **room42_B** model used to represent the BESTEST cases can be seen in Fig. 5. Several of the already presented components are interconnected in the room model. The central component is the air control volume component, modeled as a simple heat storage model. The half interior walls, roof, and floor model convective sides are connected to the air volume. The longwave radiation exchange

[1] for $\theta_{sur} = 0^\circ$, any ϕ_{sur} will have the same θ_i value.

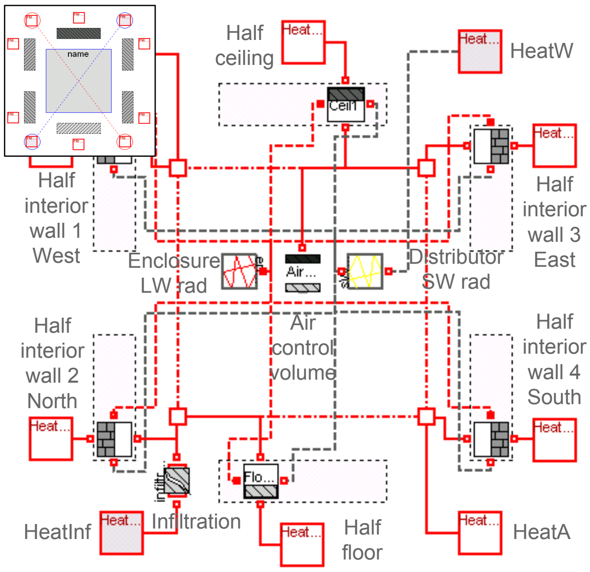

Figure 5: Diagram layer of room42_B model.

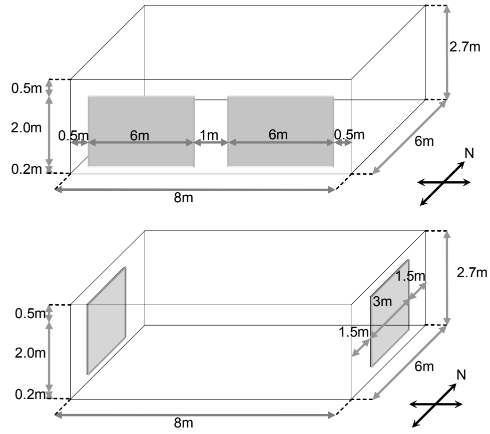

Figure 6: Basic geometry of BESTEST building with south windows (above) and with east and west windows (below).

heat flow rate is calculated in the Enclosure LW component. The heat flow rate due to the solar radiation transmitted by the windows enters into the room model through the special purpose heat connector HeatW and it is distributed in the enclosure by the Distributor SW rad model. The room model also has an infiltration subcomponent connected to the special purpose heat connector HeatInf.

4 BESTEST approach

Comparative testing is used to compare the performance of the HITLib library with the standard building simulation tools. The BESTEST approach [6] consists of a set of carefully specified cases (36 cases) for software-to-software comparisons, and program diagnostics that can be easily defined over a variety of detailed and simplified whole-building energy simulation programs. The cases go from simple to complex, and only 14 of them are for qualification. Qualification cases 600 to 650 and 900 to 990 represent a set of lightweight and heavyweight buildings that are relatively realistic with respect to their thermal characteristics. The basic geometry of the test case building is a simple rectangular single zone with no interior partitions (see Fig. 6). These test cases are implemented and evaluated with the Modelica building library and the corresponding results are compared with those of the reference whole building energy simulation tools (i.e. BLAST, DOE2, ESP, SERIRES, S3PAS, SUNCODE, TASE, and TRNSYS).

Since non shading device has been modeled cases 610, 630, 910, and 930 can not be properly modeled. Cases 650, 950 were not tested since no scheduled ventilation model was implemented and cases 960 and 990 were neither evaluated. The tested cases (see table 1) allow us to analyze the performance of the library in the aspects of basic heat transfer (case 600), east and west incidence and/or transmittance solar radiation (620 & 620-600) and setback control (640 & 640-600) for the light weight cases, and mass and/or south solar interaction (900 & 900-600), mass and/or east-west solar interaction (920 & 920-900), and mass and/or setback interaction (940 & 940-900) for the heavy weight cases.

A typical meteorological year (TMY) weather data file is provided to perform the tests, the ground modeling is not generally good, therefore a highly insulated floor has been defined in the test cases to effectively decouple the floor thermally from the ground. A ground temperature of 10 °C is applied through a heat boundary condition component (see BC1 subcomponent in Fig. 7). The infiltration component automatically correct its value according to the atmospheric pressure. The internal generated heat gains from equipment, lights, people, animals, etc. that are not related to HVAC correspond to sensible heat (no latent) and they have a value of 200W for the test cases (60% radiative, 40% convective, 100% sensible, 0% latent). The convective and radiative part of the internal gain have been implemented with heat boundary condition components (see BC2 and BC3 subcomponents in Fig. 7), where the first is directly connected with the air mass volume (inside the room model) while the second has been connected to a shortwave distributor model (inside the room model). For the shortwave internal solar distribution fractions the values

Case	Mass	Thermostat
600	Light	Deadband or 20,27
620	Light	Deadband or 20,27
640	Light	Setback
600FF	Light	free-float
900	Heavy	Deadband or 20,27
920	Heavy	Deadband or 20,27
940	Heavy	Setback
900FF	Heavy	free-float

Table 1: BESTEST qualifying cases tested

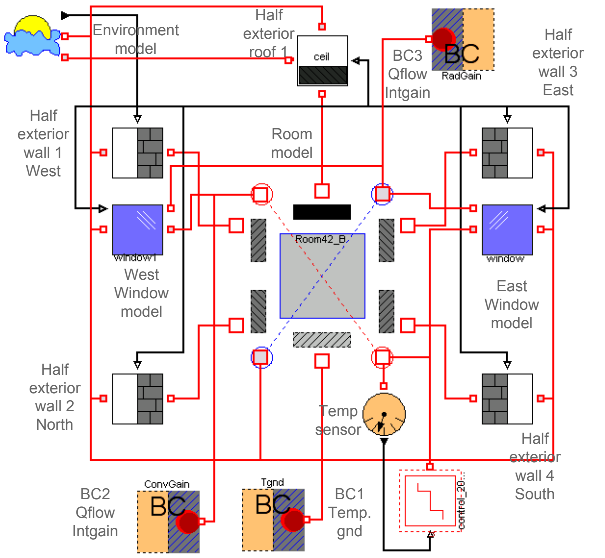

Figure 7: Dymola diagram layout of BESTEST cases 620 and 920 with east/west windows.

Deadband or 20,27	Heat=on if temp<20C Cool=on if temp>27C
Setback	23:00<time<07:00 heat=on if temp <10C 07:00<time<23:00 heat=on if temp <10C cool=on if temp>27C

Table 2: BESTEST heating and cooling thermostat control system

provided by BESTEST are used.
The heating and cooling systems are 100% convective, the thermostat is sensing only the air temperature and it is assumed that there are no latent loads. Both heating and cooling capacities are of 1000 kW and they have an effective efficiency of 100%. Two thermostat control strategies has been implemented (see Table 2),

4.1 Results

There are two types of outputs, the annual outputs defined over the whole reference year and daily hourly outputs defined over specific days of the year for certain tests.

Annual type outputs

- Annual heating and cooling loads (MWh) for all non free-float cases, see Fig. 8.
- Annual hourly peak heating and cooling loads (kW) for all non free-float cases, see Fig. 9
- Difference among annual thermal loads among the non free-float cases, see Fig. 10.
- Difference among annual hourly peak thermal loads among the non free-float cases, see Fig. 11.

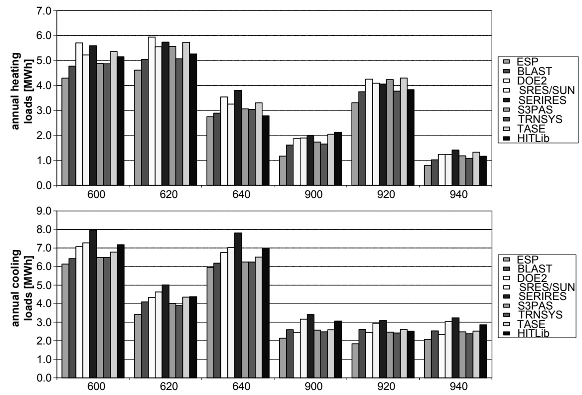

Figure 8: Annual heating loads for low mass buildings - cases 600, 620, and 640- and high mass buildings - cases 900, 920, 940- (above). Annual cooling loads for the same cases (below).

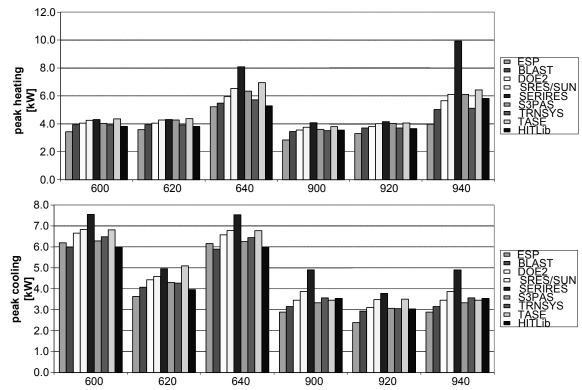

Figure 9: Annual peak heating loads for low mass buildings - cases 600, 620, and 640- and high mass buildings - cases 900, 920, 940-(above). Annual peak cooling loads for the same cases (below).

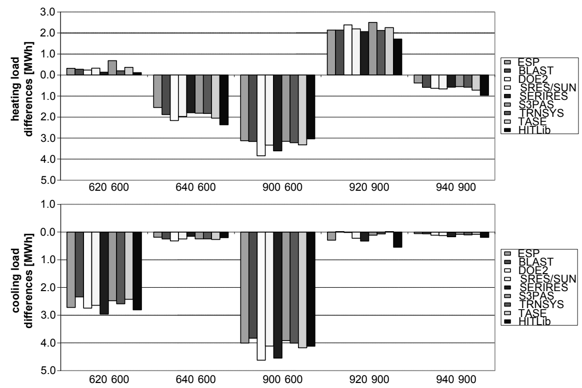

Figure 10: Annual heating load differences among the cases (above). Annual peak cooling load differences among the same cases (below).

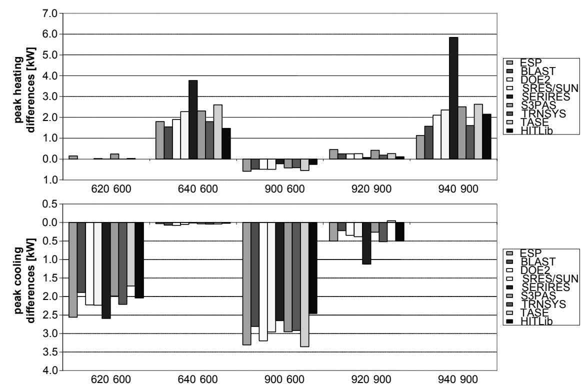

Figure 11: Annual peak heating load differences among the cases (above). Annual peak cooling load differences among the same cases (below).

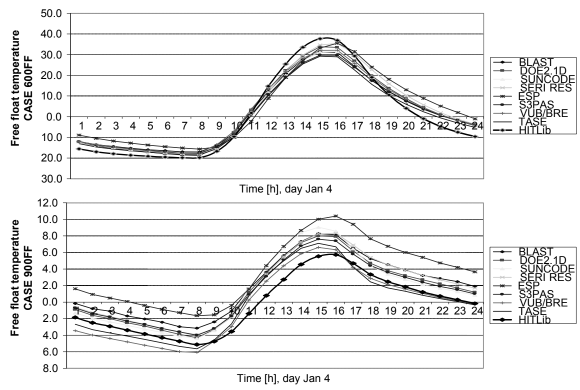

Figure 13: Hourly free float temperatures on January 4 for the case 600FF (above). Hourly free float temperatures on January 4 for the case 900FF (below).

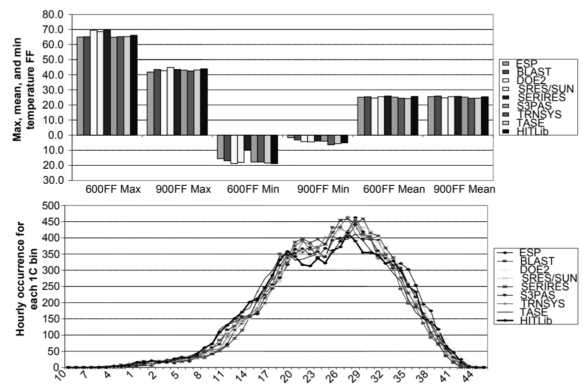

Figure 12: Maximum, mean, and minimum temperatures for the free floating cases 600FF and 900FF (above). Case 900FF temperature histogram with bins of 1C (below).

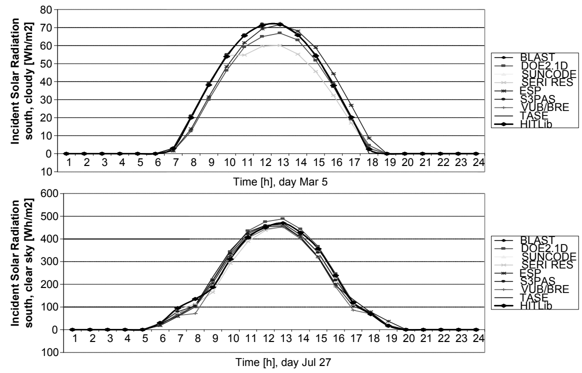

Figure 14: Hourly solar incident radiation over a south facing surface in a cloudy day, March 5 (above). Hourly solar incident radiation over a south facing surface in a clear day, July 27 (below).

- Annual hourly-integrated maximum, minimum and average indoor air temperature for all free-float cases and annual hourly-integrated indoor air temperature histogram for free-float case 900FF, see Fig. 12.

Annual hourly-integrated maximum, minimum and average indoor air temperature for all free-float cases show a good level of coincidence as well as the annual hourly-integrated indoor air temperature histogram for free-float case 900FF.

Annual heating and cooling loads for all non free-float cases show a reasonable agreement between the reference values and the values obtained with HITLib. Annual heating load for case 900 and annual cooling load for case 920 are slightly out of the range of the reference values, this does not pose a significant problem since in general for the high mass cases (series 900) there is an expected higher variability among the reference outputs. The difference among the annual thermal loads among the non free-float cases show also a good level of agreement with the reference values.

Annual hourly peak heating and cooling loads (kW) for all non free-float cases show a good level of agreement with the reference values and the time when they occur[2]. Difference among annual hourly peak thermal loads among the non free-float cases also show high coincidence with the reference values.

Daily hourly outputs

- Hourly free-float cases indoor air temperature for 600FF and 900FF (January 4), see Fig. 13.
- Hourly unshaded incident solar radiation on south surfaces in a cloudy day (March 5) and a clear sky day (July 27), see Fig. 14.
- Hourly unshaded incident solar radiation on west surface in a cloudy day (March 5) and a clear sky day (July 27), see Fig. 15.
- Hourly heating and cooling (kWh) for cases 600 and 900 (January 4), see Fig. 16.

The HITLib daily hourly outputs have a high matching with the BESTEST reference values.

[2] this is not presented here

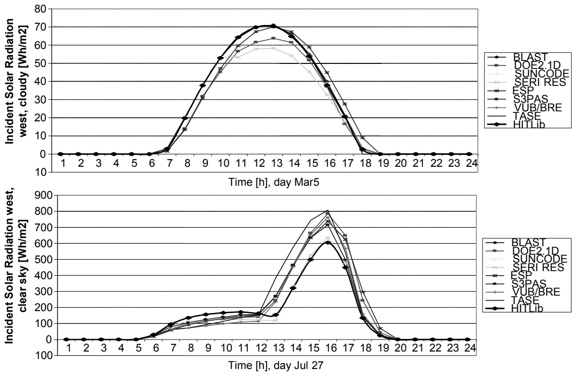

Figure 15: Hourly solar incident radiation over a west facing surface in a cloudy day, March 5 (above). Hourly solar incident radiation over a west facing surface in a clear day, July 27 (below).

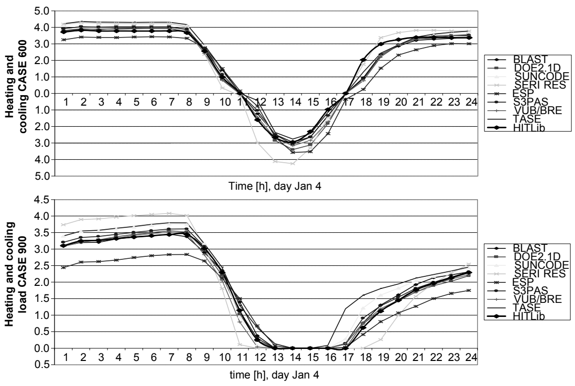

Figure 16: Hourly heating and cooling loads on Jannuary 4 for case 600 (above). Hourly heating and cooling loads on Jannuary 4 for case 900 (below).

5 Conclusions

The final goal of the library is to give intuitive blocks for modeling the building thermal response to test and develop advanced controllers for system level simulation. Modelica language seems to be an adequate language for this purpose, allowing a simple equation-based formulation of well-known building models.
BESTEST method only compares certain aspects of an energy representation of a building and many models of the new library have not been presented since they can not be evaluated (e.g. interzone convective heat flow). Additionally, not all the BESTEST qualification cases have been tested since some of them are of no interest for the library purpose (e.g. hangout shading). Nonetheless, a quality measurement in the aspects studied in the test cases can be accepted as a good starting point in the validation procedure of the library.
Many of the models used for the BESTEST are still under development but the library seems to lack of any significant modeling error. Particularly, the window model is still under revision and a more refined model addresing the multi-layer glazing cases will be developed.
The library is still under-development and many improvements are foreseen and it will be freely available in the upcoming months.

References

[1] J. A. Clarke, *Energy Simulation in Building Design*. Butterworth-Heinemann, 2001.

[2] D. B. Crawley, J. W. Hand, M. Kummert, and B. T. Griffith, "Constrasting the capabilities of building energy performance simulation programs," US Department of Energy, ESRU University of Strathclyde, SEL University of Wisconsin-Madison and National Renewable Energy Laboratory, Tech. Rep., 2005.

[3] J. A. Duffie and W. A. Beckman, *Solar Engineering of thermal processes*. Jhon Wiley and Sons, Inc., 1991.

[4] F. Felgner, S. Agustina, R. C. Bohigas, R. Merz, and L. Litz, "Simulation of thermal building behavior in modelica," in *Proceedings of the 2nd International Modelica Conference*, Oberpfaffenhofen, Germany, March 2002, pp. 147–154.

[5] M. Iqbal, *An introduction to solar radiation*. Academic press canada, 1983.

[6] R. Judkoff and J. Neymark, "International energy agency building energy simulation test (bestest) and diagnostic method," National Renewable Energy Laboratory, Tech. Rep., 1995.

[7] M. Martin and P. Berdhal, "Characteristics of infrared sky radiation in the united states," *Solar Energy*, vol. 33, pp. 321–336, 1984.

[8] T. Muneer, *Solar Radiation and Daylight Models for the Energy Efficient Design of Buildings*. Architectural press, 1997.

[9] A. Rabl, *Active Solar Collectors and their applications*. Oxford University press, 1985.

[10] R. Siegel and J. R. Howell, *Thermal Radiation Heat Transfer*, 3rd ed. Hemisphere Publishing Corporation, 1992.

[11] C. P. Underwood and F. W. H. Yik, *Modelling Methods for Energy in Buildings*. Blackwell Publishing, 2004.